THE INFLUENCE OF VISCOSITY ON THE GAS-LIQUID SLUG FLOW

Eugênio Spanó Rosa
Universidade Estadual de Campinas – Faculdade de Engenharia Mecânica – Departamento de Energia
Rua Mendeleiev, s/n - Cidade Universitária "Zeferino Vaz" - Barão Geraldo - Caixa Postal 6122 - CEP: 13.083-970 - Campinas - SP
erosa@fem.unicamp.br

Milvio Duarte
Universidade Estadual de Campinas – Faculdade de Engenharia Mecânica – Departamento de Energia
Rua Mendeleiev, s/n - Cidade Universitária "Zeferino Vaz" - Barão Geraldo - Caixa Postal 6122 - CEP: 13.083-970 - Campinas - SP
milvio@fem.unicamp.br

This work analyzes experimetally the viscosity effect on the gas-liquid structures occuring in the slug flow pattern . The experimental apparatus consists of a gas-liquid mixer located at the inlet of the test section. The test section is of a transparent acrylic pipe with 26 mm ID 23.4 m long. Two couples of fluids are tested: air-water and air-glycerin. The water viscosity is of 1 cP, and the water-glycerin mixture is of 27 cP. The lengths, speeds and frequencies of the gas-liquid structures are obtained by four measuring stations positioned along the test section. They are made of a couple of parallel wire probes and located at 127, 267, 494 and 777 diameters from the mixer. The tests are performed for the same gas-liquid flow rates allowing a straightforward comparison of the viscosity change on the flow properties. The results are presented in terms of mean values, histograms and also through correlations concerning coefficients.

Keywords. slug flow, multi-phase flow, viscosity.

1. Introduction

A gas-liquid mixture flowing through a pipe for a large flow range has its gas and liquid phases distributed intermittently along the pipe. This flow pattern is characterized by a succession of elongated bubbles flowing over a liquid film and liquid slugs that do not occur with size and frequency defined due to the interactions between bubbles and liquid slugs. The flow is represented by a sucession of unit cells composed by a liquid piston trailed by gas bubble, as seen in Fig. 1.

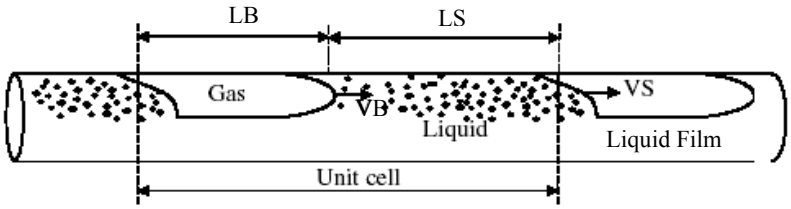

Figure 1. Intermittent flow representation using the unit cell concept.

The length, speed and frequency of the gas-liquid structures within the individual unit cells are influenced by several flow parameters such as: gas and liquid flow rates, pipe diameter, fluids density, viscosity and surface tension among others. The physical description of these parameters is done in several experimental and theoretical works. Certainly one of the most relevant is the pioneering work of Dukler and Hubard (1975). Using the concept of the unit cell, they developed a flow model based on the time and space averaged properties of the unit cell and also on the experimental observations concerned to air-water flow experiment in a 31 mm diameter pipe. The values of bubble velocity, slug and bubble lengths, pressure drop, unit cell frequency among other parameters became available. Since the original model the list of experimental and theoretical works on the subject is extense and the following reviewing articles is recommended for an overall sigh of the available experimental data, modeling work and the lose ends of the slug flow: Taitel and Barnea (1990), Fabre and Liné (1992) and Dukler and Fabre (1992). The following paragraphs cites some works which are relevant to the present paper. The bubble velocity propagation was further studied for horizontal and inclined pipes in Bendiksen (1984). Based on experimental data from air-water mixtures or mixtures with light viscosity oils and in theoretical models unit cell frequency were proposed in Gregory and Scott (1969) and in Tronconi (1990). Recently, Nadler and Mewes (1995) studied experimentally the effects of liquid viscosity on the liquid holdup of the unit cell and individually on the liquid holdup in the gas bubble and on the liquid slug. Using air-water and air and mineral oil experimental data base. Detailed statistical analysis of the slug flows has been made by Nydal et al. (1992), Grenier (1997) and Rosa et al. (2001), based on experimental work with mixtures of air and water.

The experimental and theoretical description of the slug flow is needed to accurately describe and predict the intermittent flow characteristeristics. As much challenging can be, most of the closure laws comes from experimental data using the air-water experiments. The present work further advances the analysis investigating experimentally the effect of viscosity increase on the gas-liquid structures of the slug flow. The experimental set up runs at near atmospheric pressure and uses two pair of fluids: air and water and air and glycerin/water solution with a liquid viscosity 27 times higher than the water. A straightforward comparison of the air-water and air-glycerin/water mixtures is drawn confirming some of the already known effects of viscosity increase and also disclosing new features.

2. Experimental set-up

A sketch of the experimental set-up appears in Figure 2. It includes a horizontal pipeline, storage and receiving tanks mixers, control valves, pumps, compressors and instrumentation. The test section is a 26 mm ID straight transparent Plexiglas pipeline 900 pipe diameters long, i.e., 23.4 m. Two pairs of working fluids were used: compressed air & ordinary tap water and compressed air & glycerin/water mixture, hereafter denoted just by A@W and A@G mixtures. High capacity compressors and a centrifugal pump supply the air and the liquid to the mixer installed at the entrance of the test section. The air-liquid mixer was made of two concentric tubes in which the inner tube delivers the air through small orifices in a porous plug while the liquid flows through the annular space. At the other end of the test section the mixture is discharged, without restraint, into a receiving tank open to the atmosphere (in average, 0.947 Bar and 25°C). From the receiving tank the liquid phase is transferred to the main tank, so that the total volume contained by the system adds-up to 3 m^3, ensuring a fairly constant liquid temperature during the experiment.

The air and liquid mixture is an isothermal flow at nearly atmospheric pressure. The fluids transport properties are considered as follow. The air is treated as an ideal gas. The ordinary tap water has density of 1000 kg/m^3, dynamic viscosity of 1 cP and air-water suface tension of 70 dyne/cm. The glycerin and water solution is made of 26.4% water volume in pure bi-distiled glycerin. It resulted in a mixture with density of 1190 kg/m^3, viscosity of 27 cP and air-glycerin surface tension of 32 dyne/cm. The liquid flow-rate was measured by a Micro-Motion® Coriolis mass type flow meter accurated within 1% of the measured mass flow. To measure the air flow-rate one used two Merian© laminar flow elements with reported an uncertainty of 1%. The range of air superficial velocities varied between 0.4 Sm/s to 1.7 Sm/s. The liquid superficial velocities ranged from 0.25 m/s to 1.35 m/s. The letter S in front of the unit specifies the local atmospheric condition (0.947 bar @ 21°C); otherwise it refers to the *in situ* conditions.

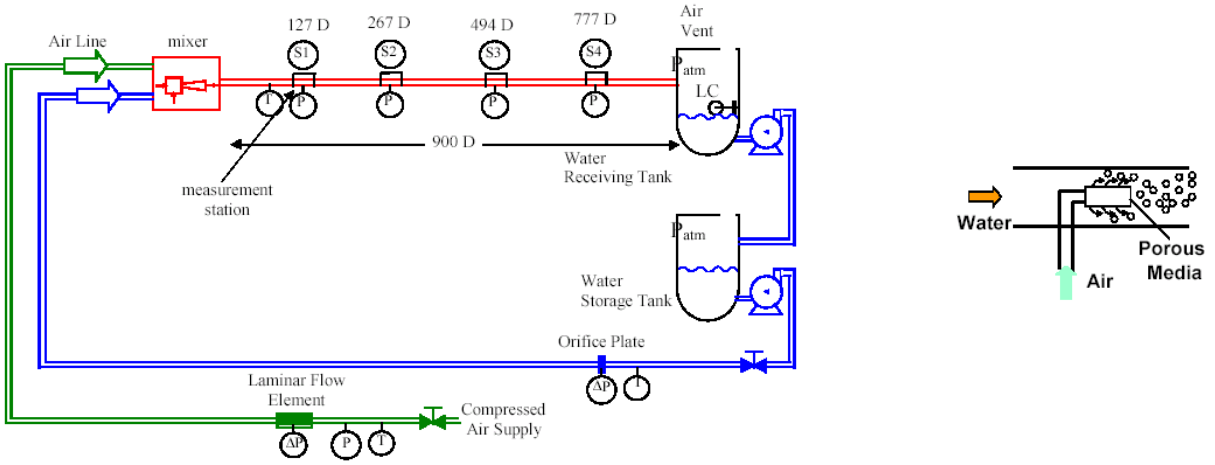

(a) (b)

Figure 2. (a) Experimental set-up, (b) gas-liquid mixer.

To identify and measure the structures of the slug flow such as the propagation velocity, the frequency, the length and the liquid film thickness, as they evolve along the pipeline were used twin double–wire conductive probes spaced 50 mm apart. These measurements were performed, simultaneously, in four measuring stations distributed along the pipeline, S1, S2, S3 and S4 located downstream of the air-liquid mixer at a distance, in terms of pipe diameters, of 127D, 267D, 494D and 777D respectively, see Fig. 2. The typical signals taken simultaneously by the twin probes, driving circuit, the sampling frequency and further treatment of the raw data are described in Rosa (2001) and Rosa (2002) and will not be reproduced here. The outcome of post-processing the experimental data is an array representing the velocity, length, liquid film thickness beneath the gas bubble and frequency of every unit cell that passed by the sensors. It is then further processed statistically, in samples not less than 300 unit cells, giving rise to average values, standard deviations, histograms and correlation coefficients.

There were taken 16 experimental data points for both A@W and A@G systems. Table 1 shows the air, the liquid and mixture superficial velocity, JG, JL and J respectively, as well as the liquid Reynolds number for each individual experimental point. The mixture superficial velocity is defined as the sum of the gas and the liquid superficial velocities, J = JG + JL and the liquid pipe Reynolds number is defined as:

$$\mathrm{Re} = J \cdot d / \nu_L , \qquad (1)$$

where ν represents the liquid kinematic viscosity and d is the pipe diameter.

Table 1. Test matrix for the Air-Water (A@W) and Air-Glycerin/Water (A@G) mixtures.

Data Point (#)	A@W				A@G			
	JL (cm/s)	JG (cm/s)	J (cm/s)	Re ($x10^3$)	JL (cm/s)	JG (cm/s)	J (cm/s)	Re ($x10^3$)
1	34	67	101	26	34	67	101	1,2
2	35	136	171	44	32	134	166	1,9
3	35	165	200	52	32	165	197	2,3
4	50	52	102	26	51	51	102	1,2
5	66	65	131	34	67	68	135	1,6
6	67	132	199	52	67	132	199	2,3
7	67	175	242	63	64	169	233	2,7
8	-	-	-	-	135	67	202	2,3
9	-	-	-	-	133	132	265	3,0

3. Experimental Results

The experimental results are presented along the following four sections. The first section displays still frames of the bubble and slug fronts. The second section shows a comparison among the averaged flow properties for both systems, A@W and A@G, taken at near fully developed condition in the measuring station 4, S#4. Sections three and four present the probability density functions, pdf, and the correlation functions, R, of some selected flow variables.

3.1. Images

The photographs in Figure 3 come from frozen frames of a black and white high-speed digital video camara CCD recorded at a shutter speed of 1:10000 seconds, 494 diameters downstream of the concentric mixer, station S3. They show the measuring station with approximately four pipe diameters long. As additional information, the frames show two straight and vertical bright lines. They are the twin parallel gold wires from the conductive probe, Rosa (2002).

For comparison purpose both pictures were taken at the same liquid and gas velocities, JL and JG of 67 cm/s represented by the experimental point 5 in Table 1. Figures 3 (a) and 3 (b) represent the pictures for the A@W and A@G systems, respectively. They bring qualitative information regarding the bubble shape and the amount of air in the liquid slug. For the A@W system, the bubble nose stays close to the top wall due to the gravity pull, the liquid film thickness beneath the air bubble is less than half pipe diameter, the liquid slug has negligible air content with a front in a stair case shape. On the other hand for the A@G system, the bubble nose shifts toward the pipe centerline, the liquid film beneath the bubble is considerable thicker than the first case, liquid piston following the bubble is not aeraded and its front also has a staircase shape.

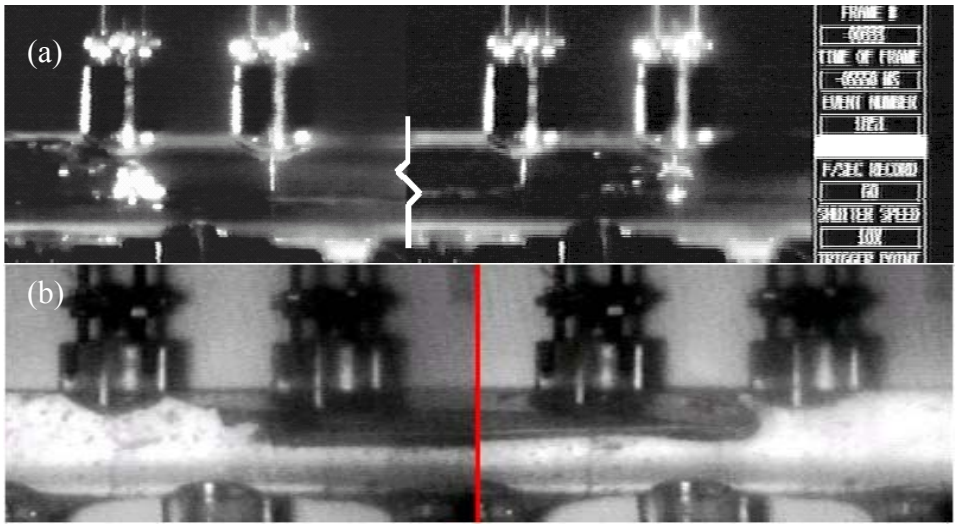

Figure 3. Experimental point # 5 (JL=67 cm/s, JG=67 cm/s). Still frames taken at 494 D downstream the gás-liquid mixer, S#3. Bubble and slug fronts for A@W system (3-a) and A@G system (3-b).

Visual records of the whole test matrix reveals that the slug fronts have always a stair case shape for both systems, A@W and A@G. But in particular for the A@W and A@G mixtures, points #1, #4 and #5 do not show appreciable gas

content within the liquid slug. The significance of this information concerns with the criteria of slug flow to plug flow proposed by Ruder and Hanratty (1989). These two subregimes of the intermittent gas flow differs in several aspects, the plug flow is found at very low gas velocities with elongated bubbles and having the bubble tail in a staircase shape with non-aerated trailing liquid slugs. On the other hand, the slug flow occurs at high velocities with the liquid slug front assuming shape as a sudden liquid expansion with aerated liquid slugs. The experimental data reveals the existence of staircase shape with and without aeraeted liquid pistons.

3.2 Mean Values

The farthest measuring station from the gas-liquid mixer is S4, located 777 pipe diameters downstream. It is taken as a reference station where the flow properties are regarded as stationary. That is, the velocities, the lengths and the frequencies do not change as quick as they used change when the gas-liquid flow is near the mixer. Due to this property, S4 was choosen to display the mean values of liquid slug and buble lengths, LS and LB; the unit cell frequency, f; and the bubble front velocity, VB.

Figure 4(a) displays the averaged liquid slug length in terms of pipe diameters, D, as a function of the superficial mixture velocity, J for both systems, A@W and A@G. As remaked by Taitel and Barnea (1990) and also by Dukler and Hubard (1975) the lengths of the liquid slugs are relatively insensitive to the gas and liquid velocities. In fact Fig. 4(a) bears the affirmative above. The ratio LS/D for the A@W and A@G systems stayed nearly constant thru all the tests at values of 16 and 10, respectively. The viscosity increase brings a LS/D decrease as observed along the tests. It apparently contradicts the affirmative that LS stays fairly constant for a given pipe diameter, Taitel and Barnea (1990).

Figure 4(b) shows the averaged bubble length in terms of pipe diameters, D, as a function of the gas to liquid superficial velocity ratio. Both systems, A@W and A@G, exhibits a linear growth of LB/D with JG/JL but the growth rate for the A@W system is bigger than the A@G system. Considering the gas content within the unit cell is the same for both cases; the small length for A@G is possible due to the increase in gas content of the liquid slug of the A@G.

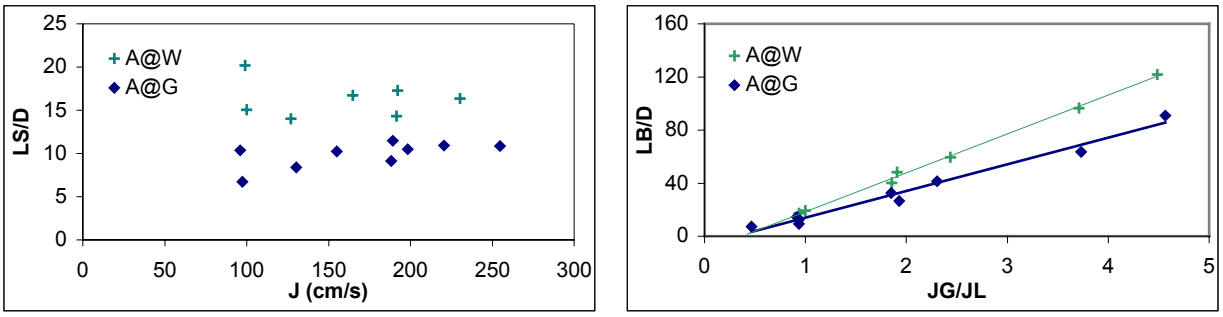

(a) (b)

Figure 4. (a) Liquid slug length to pipe diameter ratio, LS/D, as a function of the mixture velocity, J; (b) bubble lenght to pipe diameter ratio, LB/D as a function of the gás to liquid velocity ratio, JG/JL.

Figure 5(a) displays the dimensionless unit cell frequency, fD/JL, as a function of the liquid quality, λ defined as $\lambda = JL/J$. The dimensionless parameters for f and J are largely employed in the available correlation frequency formulas, as reviewed in Taitel and Barnea (1990). As seen in Fig. 5(a), the viscosity increase leads to an increase on the cell frequency considering the same JL and JG velocities. This frequency increase is justified since the lengths of the liquid slug and gas bubble decrease when viscosity increases. Since the liquid and gas content are the same for both cases the decrease in length is balanced by the increase in frequency to keep up with the mass balance. Another remark about Fig. 5(a), is the fact that the dimensionless frequency shows sensitivity to the liquid viscosity while the available correlation formulas do not exhibit any explicity dependency on the liquid viscosity. Employing a different approach from the frequency prediction methods coted in Taitel and Barnea (1990), there is the one proposed by Tronconi (1990). The cells frequencies are inversely proportional to the period of finite amplitude wave prior to the pipe bridging. Although not shown here, a straithforward comparison of the frequency estimates, either using Tronconi's method or the ones based on the liquid quality, are not favorable to the A@G experimental frequency data.

Figure 5(b) shows the nose velocity of the elongated bubble in a presence of a train of slug units. Based on experiments with an isolated bubble Nicklin et al (1962) proposed a linear "drift-flux like" relationship to determine the bubble nose velocity, VB,

$$VB = C_0.J + V_\infty \quad (2)$$

where the constants C_0 and V_∞ are associated, in order, to the phase's distribution and to the bubble drift velocity in a fluid at rest. Its usage for a train of bubbles is straightforward; the experimental values of C_0 and V_∞ and the the linear regression coefficient, R^2 are in Table 2. As observed from Fig. 5(b) the bubble velocity is very well correlated by Eq. (1) for both systems: A@W and A@G also, the viscosity increase results in an increase for the C_0 coefficient from 1,17 to 1,19. The accepted interpretation of Eq.(1) is that the bubble propagates at a rate slightly less than the non-perturbed maximum liquid velocity, Polonsky (1999). For turbulent regimes with 1/7 power profiles for the liquid slug, the center

velocity is about 1,22 of the averaged liquid velocity which is approximately close to the experimentally determined value of 1,17 for the A@W which has pipe Reynolds numbers ranging from 26000 to 65000. On the other hand considering liquid slugs flowing in the laminar regime, the parabolic profile renders a center velocity twice the averaged liquid velocity. Looking at the A@G data base, with pipe Reynolds numbers ranging from 1200 to 3000, the measured C_0 of 1,19 does not support the given interpretation otherwise it would had to be close to 2,0 instead. One of the causes for the deviation on C_0 constant for laminar regime is the fact that the laminar profile was not fully established. Pinto (1998) measured for laminar flow regime C_0 of 2 for vertical slug flow, but they succeeded only for well established parabolic profiles.

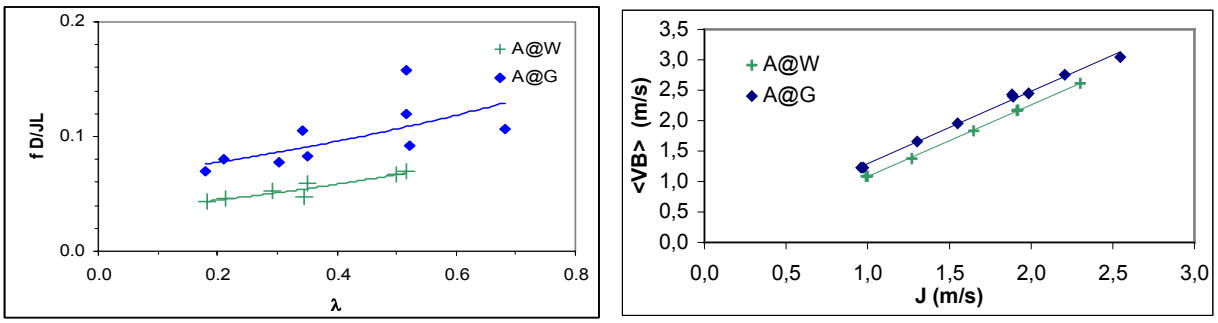

(a) (b)

Figure 5. (a) Dimensionless cell frequency against the liquid quality, λ = JL/J. (b) Bubble front velocity, VB, against the mixture superficial velocity, J.

Table 2. The C_0 and V_∞ constants resultant from a least square fit of the experimental data.

	C_0	V_∞	R^2
A@G	1,19	0,107	0,9941
A@W	1,17	-0,090	0,9994

Figure 6 brings the estimated averaged bubble void fraction, ε_B, as a function of the gas superficial velocity, JG. The averaged bubble void fraction is defined as the ratio between the gas volume within the elongated bubble region divided by the equivalent pipe volume, $\varepsilon_B = V_{G,B}/LB.A$ where $V_{G,B}$ is the gas volume within the elongated bubble and A is the pipe cross section area. The experimental method do not determine ε_B directly but estimates it by measuring the liquid film thickness beneath the bubble and, considering a plane gas-liquid interface, evaluates the ratio between the area occupied by the gas and the pipe cross section area. The average ε_B results from the average of the area ratios taken along the bubble length. As seen in Fig. 6(a), the bubble void fraction increases with the increase of JG and the bubble void fraction for the A@W mixture is always bigger than the one A@G mixture. The data are in agreement with the experimental measurements of Nadler and Mewes (1995). But the differences in the bubble void fraction may not be only due to the viscosity differences between the liquid phases, but also due to the liquid density and surface tension differences between the mixtures A@W and A@G.

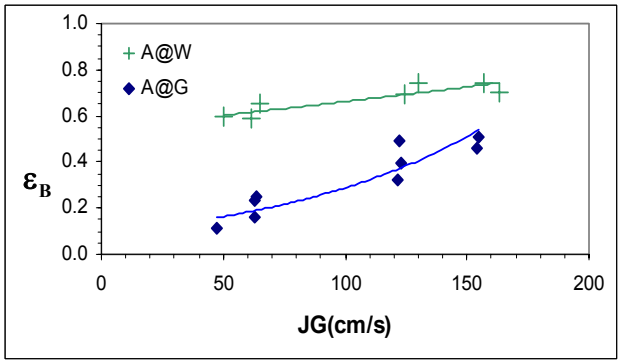

Figure 6. Averaged bubble void fraction, ε_B, against gas the superficial velocity;

3.3. The Probability Density Functions

Figure 7 shows the axial evolution along the test section of the probability density functions of the slug front velocity, VS and also of the bubble front velocity, VB taken at the experimental point #1, (JL=33 cm/s & JG=67 cm/s).

The left column in Figure 7 regards to the A@W mixture while the right column represent the data from the A@G mixture. The symbols S1 thru S4 stands for data taken at the measuring stations S1 thru S4 as reported in Fig. 1. For the A@W mixture the slug front velocities have nearly uniform pdf at S1. As the flow evolves downstream the mixer the pdf changes to an almost log-normal pdf at S3. It further decrese its mean value and standard devition at S4. It clearly shows that the population of the fast moving slugs at S1 desapears at S4 indicating a strong bubble to liquid slug interactions between S2 and S3. On the other hand, the bubble front velocity starts with a higher mean value and standard deviation to get down to a nearly stable pdf at S3 and S4 reducing its mean value and standard deviation. Similarly the fast moving bubble population desapears from S1 to S3 suggesting that the higher bubble speeds are associated with the slug formation processes and tend to fade out as the flow march downstream the pipe. A different trend is observed for the A@G mixture. In fact, the A@G lacks of the influence of the formation process since the pdf S1 through S4 are almost coincident for both VS and VB. It suggests that the increase in the liquid viscosity enhance the influence of the bubble to liquid slug interactions, indicating that most of the interaction for the A@G occurred in a distance within the gas-liquid mixer and S1.

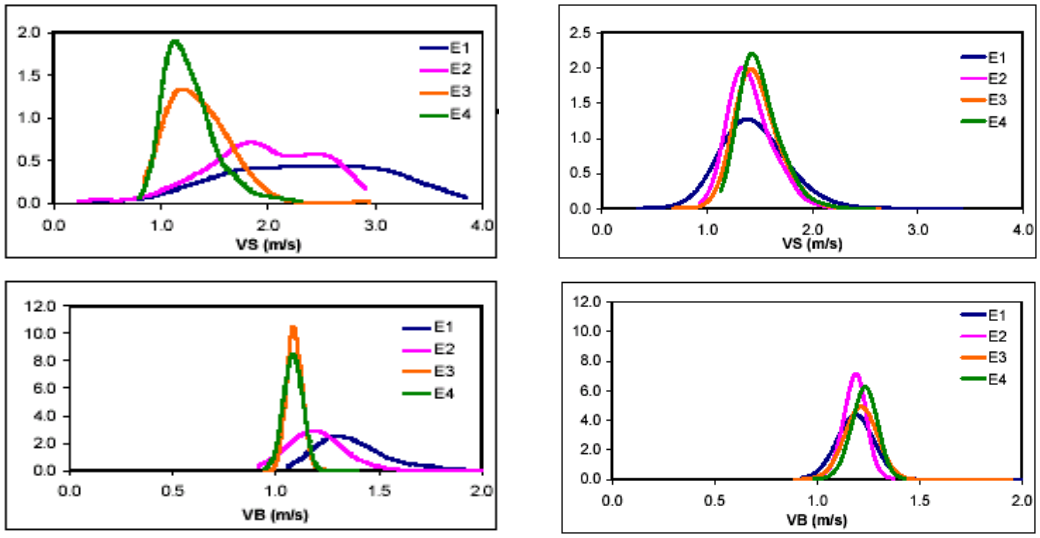

Figure 7. Density probability functions at measuring stations S1 thru S4 for VS and VB taken at point #1 (JL = 33 cm/s & JG = 67 cm/s). The lef column regards to the data of A@W while the right to the A@G mixture.

3.4. Correlation coefficient, R_{xy}

This section presents the correlation coefficient between two variables, Rxy. It is defined accordingly to Eq. (3):

$$\langle x\rangle = \frac{1}{N}\sum_{i=1}^{N} x_i \qquad S_x = \sqrt{\frac{1}{N-1}\sum_{i=1}^{N}\left[\langle x\rangle - x_i\right]^2} \qquad R_{xy} = \frac{\frac{1}{N-1}\sum_{i=1}^{N}\left[\langle x\rangle - x_i\right]\cdot\left[\langle y\rangle - y_i\right]}{S_x \cdot S_y}, \tag{3}$$

where <x> stands for the mean value and Sx to the standard deviation of x.

It is investigated the degree of linear correlation for two specific cases: a) slug front velocity, VS, and the length of the liquid slug following it, LS, and b) the length of the liquid slug, LS and the velocity difference between the slug front and the trainling bubble, VS-VB. The first case seeks if the fastest slug fronts happen with the lengthiest liquid slugs and the second case seeks if the smallest slug lengths happen for the greatest velocity difference. They are manifestations of the Nicklin kinematic law, Eq. (2).

Figure 8 shows a scatter plot of cases (a) and (b) for experimental data taken at the measuring station S4 for point #2 (JL = 33 cm/s e JG = 133cm/s). The left column in Fig. 8 refers to the A@W and the right column to the A@G. The top and bottong rows apply to the VS to LS and LS to VS-VB correlation coefficients. The top row of Fig. 8 reveals, by visual inspection, a degree of correlation ($R_{VS,LS}$ = 0.88) for A@G while for the A@W is very weak, ($R_{VS,LS}$ = 0.28). It indicates that for the A@G mixture the fastest slug front velocities are followed by the longest slugs but the same is not true for the A@W mixture. The botton row of Fig. 8 also shows by visual inspection that the slug length and the velocity difference have correlation for A@G ($R_{LS,VS\text{-}VB}$ = -0.88) but not for the A@W ($R_{LS,VS\text{-}VB}$ = -0.25). It shows for A@G system that the length of the liquid slugs grows as the velocity difference decreases.

The correlation analysis is extended to the whole experimental data points in Fig. 9. Figure 9(a) discloses the correlation coefficients for the slug front velocity and the slug length and Fig. 9(b) portraits the correlation coefficient for the slug length and the velocity difference between the slug front and the trailing bubble. The trend observed in Fig. 8 repeats for the experimental data set. It is observed a higher degree of correlation for the A@G mixture while the A@W exhibits weak correlation coefficients. Execptions are experimental points #1, #4 and #5. Perhaps one the reasons for this behavior is that the distance of S4 is not enough to the entrance effects die away of and the pdf of the

flow structures became stationary in space indicating the existence of a fully developed state. Also, coincidently the points #1, #4 and #5 exhibits non-aereted liquid pistons. This matter should be further investigated.

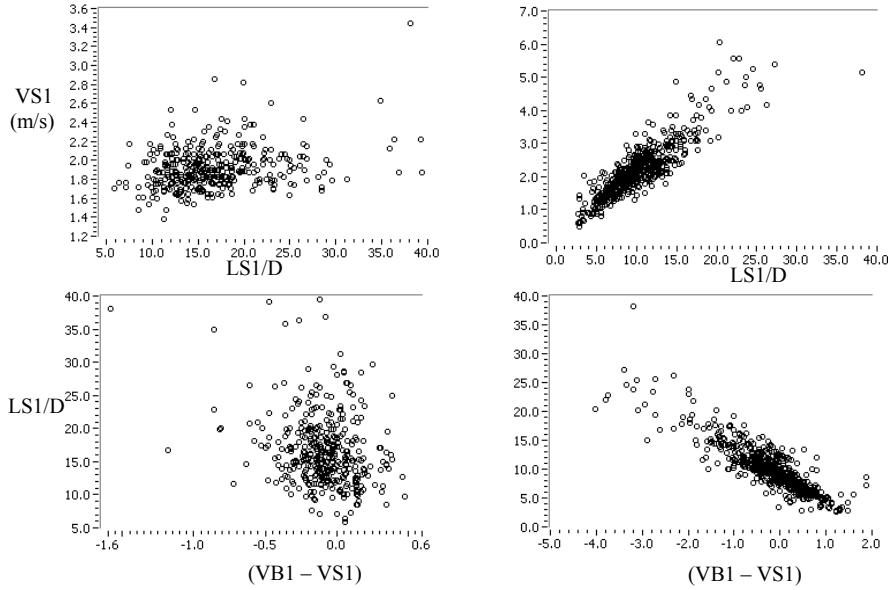

Figure 8. Scatter plot between the slug front velocity, VS, and the slug length, LS, top row and slug length and velocity difference VS-VB, botton row. Data taken at measuring station E4 for (JL = 33 cm/s e JG = 133 cm/s). The left and right columns aplly to the A@W and A@G mixtures respectively.

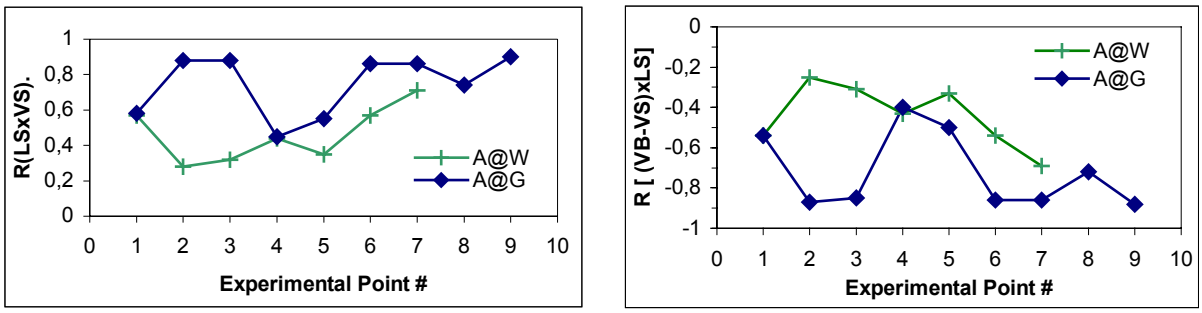

(a) (b)

Figure 9. Correlation coefficient for experimental data taken at E4 for the whole data points. (a) correlation coefficient for the slug front velocity and the slug length; (b) correlation coefficient for the slug length and the velocity difference, VS-VB.

4. Conclusions

The experimental data show that the viscosity increase causes changes in the gas-liquid flow structures of the slug flow pattern.

The experiment is limited to liquid viscosities of 1 cP and of 27 cP. As the liquid viscosity changed its density and surface tension also changed from 1000 kg/m^3 to 1190 kg/m^3 and from 70 dyne/cm to 32 dyne/cm. Despite of the change 1:27 in the liquid viscosity, it should be remarked that some of the experimental result may also be influenced by the small changes in the liquid density and surface tension.

The viscosity change did not have effect on the staircase bubble tail shape. It is present in the A@W and A@G systems with aerated and non-aerated liquid pistons. The averaged length of the slug and of the bubble reduced with the increase of the liquid viscosity. On the other hand, the unit frequency of the viscous liquid is higher than the less viscous liquid. The front bubble velocity has a linear behavior with the mixture velocity and is almost coincident for both A@W and A@G. Eventhough one may say that the viscosity increase leads to a mild increase on the front bubble velocity. The averaged bubble void fraction also is sensitive to the viscosity change. The data shows for the A@G mixture a decrease on the bubble void fraction as compared with the A@W misture.

The viscosity increase also manifests itself on the pdf evolution of the VS and VB along the pipe. The data suggest a stronger coupling between the gas bubble and liquid piston when the viscosity increases. The pdf for the A@G are almost stationary indicating weaker traces of the slug formation process. The same does not apply to the A@W mixture.

The pdf show large variations as the flow evolves downstream the gas-liquid mixer indicating the flow takes more length (or time) to establish a fully developed state.

Finally, the correlation coefficient between the slug length and velocity or slug length and velocity difference are also sensible to the liquid viscosity. The experimental data from the A@G mixture do show linear correlation among the variables mentioned above, but the A@W exhibits weak correlation coefficients for the same cases. Further experimental analysis has to be carried on to check if there is lack of correlation coefficients for A@W or if the pipe length was not enough to establish a fully developed state.

5. References

Bendiksen, K.H., 1984, "An Experimental Investigation of the Motion of Long Bubbles in Inclined Tubes", Int. J. Multiphase Flow, Vol. 10, pp. 467-483.

Dukler, A.E. and Fabre, J., 1992, "Gas-Liquid Slug Flow Knots and Loose Ends", Third International Workshop on Two-Phase Flow Fundamentals.

Dukler, A.E. and Hubbard, M. G., 1975, "A Model for Gas-Liquid Slug in Horizontal and Near Horizontal Tubes", Ind. Eng. Chem. Fundam., Vol. 14, n.4, pp. 337-347.

Fabre, J. and Liné, A., 1992, "Modeling of Two-Phase Slug Flow", Annual Review of Fluid Mech., 24:21-26.

Gregory, G.A. and Scott, D.S., 1969, "Correlation of Liquid Slug Velocity and Frequency in Horizontal Cocurrent Gas-Liquid Slug Flow", AIChE J., 15, 933-935.

Grenier, P., 1997, "evolution des Longuers de Bouchons Écoulement Intermittent Horizontal", Ph.D thesis, Institut National Polytechnique de Toulouse, France.

Nadler, M. and Mewes, D.; 1995, "Effects of the liquid viscosity on the phase distributions in horizontal gas-liquid slug flow", Int. J. Multphase Flow, 21,2, 253-266.

Nicklin, D.J., Wilkes, J., and Davidson, J.F., 1962, "Two phase flow in vertical tubes", Trans. Inst. Chem Engng, vol.40, pp61-68.

Nydal, O.J., Pintus, S., Andreussi, P., 1992, "Statistical Characterization of Slug Flow in Horizontal Pipes", Int. J.
Multiphase Flow 18, 439-453.

Taitel, Y. and Barnea, D., 1990, " Two phase slug flow", In Advances in Heat Transfer (editted by Harnett, J.P. & Irvine, T.F. Jr) vol. 20, pp 83-132, Academic Press.

Pinto, A.M.F.R.; Pinheiro, C.M.N. and Campos J.B.L.M., 1998, "Coalescence of two gas slugs rising in a co-current flowing liquid in vertical tubes", Chem. Engng. Sci, 53, 16, pp. 2973-2083.

Polonsky, S.; Shemer, L. and Barnea, D.; 1999, "The relation between the Taylor bubble motion and the velocity field ahead of it", Int. J. Multphase Flow, 25, pp. 957-975.

Rosa, E.S., Morales, E.R., Melo, A.I.; Freire R. and França, F.A., 2001," The evolution of slug flow", Cobem 2001,

Rosa, E.S., 2002,"Flow Structure in the Horizontal Slug Flow", 9th Brazilian congress of Thermal Engineering and Sciences.

Ruder, Z. and Hanratty, T.J.; 1989, "A definition of gas-liquid plug flow in horizontal pipes", Int. J. Multiphase Flow, 16,2, 233-242.

Tronconi, E., 1990. "Prediction of Slug Frequency in Horizontal Two-Phase Slug Flow", AIChE J. 36, 701-709.

6. Acknowledgement

This work was funded by the FINEP-CTPETRO and PETROBRAS under the grants n. 65.2000.0043.00 and n. 2101034100 respectively. The authors are grateful to Dr. Fagundes Neto from Petrobras, for the useful suggestions and constant encouragement.

7. Copyright Notice